The Plant Journal (2008) **53**, 790–801 doi: 10.1111/j.1365-313X.2007.03375.x

ROXY1 and *ROXY2,* two Arabidopsis glutaredoxin genes, are required for anther development

Shuping Xing[1] and Sabine Zachgo[1,2,*]
[1]*Max Planck Institute for Plant Breeding Research, 50829 Cologne, Germany, and*
[2]*Department of Botany, University of Osnabrück, 49076 Osnabrück, Germany*

Received 23 August 2007; revised 25 October 2007; accepted 31 October 2007.
[*]For correspondence (fax +49 221 5062113; e-mail szachgo@mpiz-koeln.mpg.de).

Summary

Glutaredoxins (GRXs) are small oxidoreductases that are involved in various cellular processes and play a crucial role in responses to oxidative stress. Three GRX subgroups exist in plants, and GRXs with active sites of the CPYC and CGFS types are common to pro- and eukaryotes. In contrast, GRXs with the CC type motif have so far only been identified in land plants. Here, we report that the two CC-type GRXs *ROXY1* and *ROXY2* together control anther development in *Arabidopsis thaliana*. Single *roxy1* and *roxy2* mutants are fertile and produce normal anthers. However, *roxy1 roxy2* double mutants are sterile and do not produce pollen. Strikingly, abaxial and adaxial anther lobe differentiation are differently affected, with early lobe differentiation being defective in the adaxial lobes, whereas later steps during pollen mother cell differentiation are disrupted in the abaxial lobes. Expression studies show that *ROXY1* and *ROXY2* are expressed with overlapping patterns during anther development. Lack of *ROXY1* and *ROXY2* function affects a large number of anther genes at the transcriptional level. Genetic and RT-PCR data imply that *ROXY1/2* function downstream of the early-acting anther gene *SPOROCYTELESS/NOZZLE* and upstream of *DYSFUNCTIONAL TAPETUM1*, controlling tapetum development. Mutagenesis of a conserved glutathione-binding glycine in the ROXY1 protein indicates that CC-type GRXs need to interact with glutathione to catalyze essential biosynthetic reactions. Analysis of these two novel anther genes indicates that redox regulation, as well as participating in plant stress defense mechanisms, might play a major role in the control of male gametogenesis.

Keywords: Arabidopsis, glutaredoxin, anther development, tapetum, gene expression, redox regulation.

Introduction

Glutaredoxins (GRXs) are small, ubiquitous oxidoreductases that mediate the reversible reduction of intracellular disulfide bonds. GRXs reduce disulfides using conserved cysteines located in active site motifs, and depend on glutathione (GSH) for reduction of the oxidized form (reviewed by Buchanan and Balmer, 2005; Fernandes and Holmgren, 2004). These oxidoreductases are involved in a large variety of cellular processes, and play a major role in defense against oxidative stress.

The *Arabidopsis thaliana* GRX family comprises 31 members, which fall into three subgroups (Rouhier *et al.*, 2006). The GRXs of the CPYC and CGFS subgroups occur ubiquitously, whereas GRXs of the CC-type subgroup have so far only been identified in land plants (Lemaire, 2004). Comparison of GRX subgroup composition in evolutionarily informative plant species revealed that the CC type, but not the other GRX groups, expanded during the evolution of land plants (Xing *et al.*, 2006). The existence of a disproportionately large subgroup of CC-type GRXs in angiosperms raises the question as to whether their functions might have been integrated into crucial processes controlling higher plant development.

The recent isolation of the first plant CC-type GRX mutant from Arabidopsis, *roxy1*, provides strong evidence for this notion, as the phenotype of this mutant reveals a function for the GRX in flower development. *roxy1* mutants initiate fewer petals than wild-type plants, and later petal morphogenesis is often aberrant (Xing *et al.*, 2005). Here, we show that *ROXY1*, together with its closest homolog, *ROXY2,* are required for anther development.

The Arabidopsis anther is a bilaterally symmetrical four-lobed structure that produces the pollen. Each lobe develops

from successive divisions of sub-epidermal archesporial cells formed in the anther primordium that give rise to three morphologically distinct cell layers. The endothecium, middle layer and tapetum surround the pollen mother cells (PMCs) that will undergo meiosis and thereby form the haploid microspores (Sanders *et al.*, 1999). The tapetum is a source for nutrients and plays an indispensable role during further microspore maturation.

To date, only a few early anther genes have been identified by mutant analysis. In *sporocyteless*/*nozzle* (*spl*/*nzz*) mutants, sporogenous cell formation is impaired and *bam1 bam2* mutants produce extra PMCs at the expense of normal anther somatic cells. This indicates that the *SPL/NZZ* gene promotes sporogenous cell formation, and *BAM1/2* promote somatic cell formation (Hord *et al.*, 2006; Schiefthaler *et al.*, 1999; Yang *et al.*, 1999). Other mutants, such as *excess microsporocytes1*/*extra sporogenous cells* (*ems1*/*exs*), *tapetum determinant1* (*tpd1*) and *somatic embryogenesis1/2* (*serk1/2*), completely lack the tapetum layer but instead produce excess PMCs that fail to complete meiosis, showing that *EMS1/EXS*, *TPD1* and *SERK1/2* function in the control of tapetum identity (Albrecht *et al.*, 2005; Canales *et al.*, 2002; Colcombet *et al.*, 2005; Yang *et al.*, 2003; Zhao *et al.*, 2002). Genetic data indicate that *EMS1/EXS* and *TPD1* act in the same pathway (Ma, 2005; Yang *et al.*, 2003) and function upstream of *DYSFUNCTIONAL TAPETUM1* (*DYT1*), a positive regulator of tapetum differentiation that is required for pollen formation (Zhang *et al.*, 2006).

Loss of *ROXY1* and *ROXY2* functions results in defects in sporogenous cell formation in adaxial anther lobes, whereas later stages such as PMC and tapetum differentiation are affected in abaxial lobes. These data indicate that, in addition to functioning in stress responses, the activities of glutaredoxins are also required for normal development of male reproductive plant organs and gametophytes.

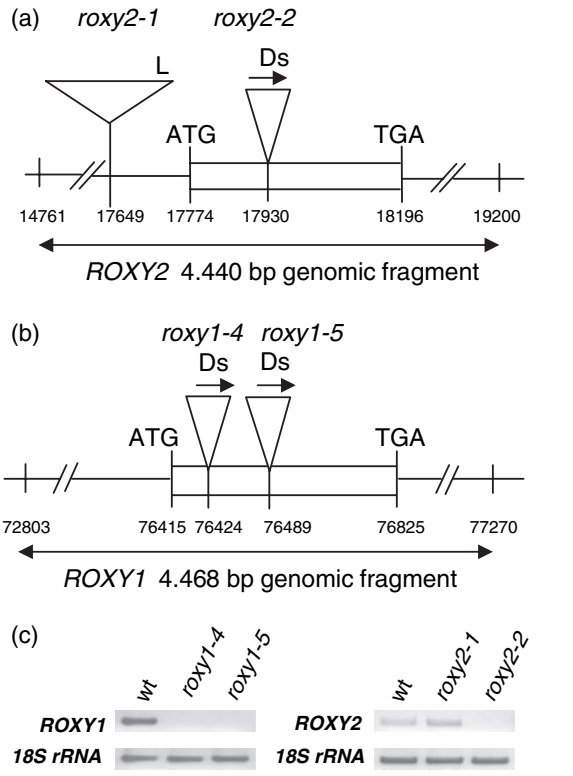

Figure 1. Isolation of *roxy2* and *roxy1* mutants.
(a) Structures of *roxy2* alleles in Col-0 (*roxy2-1*) and Nössen (*roxy2-2*) backgrounds. Numbering of the coordinates is based on the BAC clone MUA 22 containing the *ROXY2* gene.
(b) Structures of two *roxy1* alleles in the Nössen background. Numbering of coordinates is based on the BAC clone F1C9 containing the *ROXY1* gene.
(c) Comparison of *ROXY1* and *ROXY2* expression in inflorescences from wild-type and mutant lines by RT-PCR. As a control, 18S rRNA was amplified.
L, left T-DNA border; Ds, transposon; arrows indicate the Ds orientation.

Results

Mutant isolation and characterization

Intrigued by the finding that the *roxy1* mutant exhibits an aberrant petal phenotype, and forms on average 2.5 rather than four petals, we analyzed the function of its closest homolog, *At5g14070* (Xing *et al.*, 2006), which was named *ROXY2* (GenBank accession EU332351). The two CC-type GRX products are 71% identical and share a CCMC active site motif.

Two *ROXY2* mutant lines were characterized (Figure 1a). The *roxy2-1* line, carrying a T-DNA insertion localized 123 bp upstream of the putative ATG start codon, was obtained from the SALK T-DNA collection (Col-0 ecotype). The *roxy2-2* mutant, derived from the RIKEN collection (Nössen ecotype), carries a Ds insertion in the sole exon of *ROXY2*. Neither of these alleles causes any obvious phenotype in single mutants. Therefore, *roxy1 roxy2* double mutants were constructed to reveal redundant functions. As RT-PCR experiments detected *ROXY2* transcripts in the *roxy2-1* allele, further analyses were conducted using the *roxy2-2* allele, which represents a knockout mutant (Figure 1c). All three of the previously described alleles of *roxy1* are in the Col-0 background (Xing *et al.*, 2005). In order to avoid complications caused by crossing two ecotypes, two additional null mutants of *roxy1* in the Nössen background, *roxy1-4* and *roxy1-5*, were obtained from RIKEN (Figure 1b,c). These *roxy1* mutants have a slightly weaker petal phenotype compared with the Col-0 alleles, and develop 3.0 petals on average (Table S1). No other obvious phenotypes outside the floral context were observed.

roxy1 roxy2 *double mutants display defects in fertility*

Strikingly, seven of 108 F_2 plants derived from a cross between the two null mutants *roxy1-5* and *roxy2-2* were sterile. Genotyping confirmed that this phenotype was

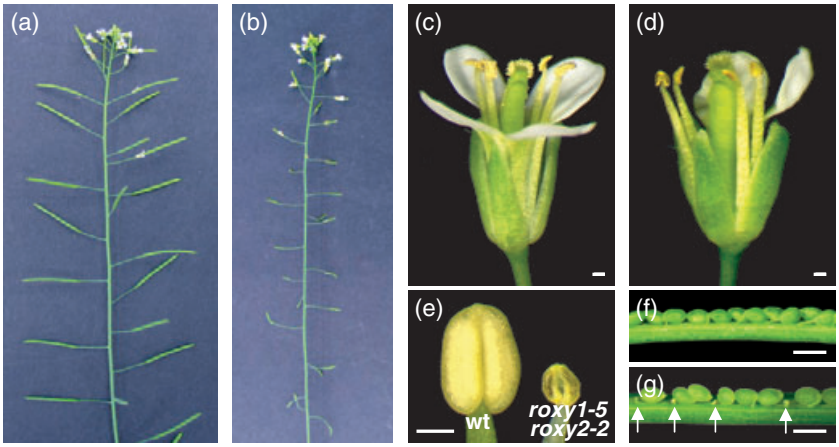

Figure 2. The *roxy1 roxy2* phenotype.
(a) Wild-type inflorescence with normal seed set in siliques.
(b) *roxy1-5 roxy2-2* inflorescence with small siliques lacking seeds.
(c) Wild-type flower showing dehisced anthers with pollen grains. Stigmatic papillae are topped with pollen grains.
(d) *roxy1-5 roxy2-2* flower showing anthers without pollen grains.
(e) Normal wild-type anther just before dehiscence (left) and a *roxy1-5 roxy2-2* anther (right) at an equivalent stage.
(f) Dissected silique from a wild-type cross, showing normally developed ovules 8 days after pollination.
(g) A *roxy1-5 roxy2-2* silique dissected 8 days after pollination with wild-type pollen. Aborted ovules are indicated by arrows.
Bars = 200 μm.

restricted to double mutants that, in addition to producing a reduced number of petals, also failed to elongate their siliques and did not set seed (Figure 2b). Additionally, anthers were smaller and did not produce pollen (Figure 2d,e). In wild-type flowers, anthers are grouped around the carpel at the time of dehiscence and deliver their pollen to the stigma (Figure 2c). In *roxy1-5 roxy2-2* flowers, anthers are arbitrarily positioned and often do not face the carpel (Figure 2d).

Failure to set seed is not solely due to lack of pollen production, because pollination of *roxy1-5 roxy2-2* pistils using wild-type pollen still yielded 21.7% aborted ovules (Table 1 and Figure 2g). In wild-type control crosses, only 2.4% of the ovules failed to develop into seeds. Crosses performed with wild-type pollen applied to the carpels of *roxy2-2* single mutants resulted in wild-type-like siliques (Table 1 and Figure 2f). These findings indicate that *ROXY1* and *ROXY2* also participate – although to a lesser degree than observed for anthers – in controlling female organ development.

An identical sterility phenotype was observed for *roxy1-4 roxy2-2* double mutants. Furthermore, a 4440 bp *ROXY2* genomic fragment (Figure 1a) rescues the sterility phenotype of the double mutant (Figure S1). Given these observations, we conclude that the fertility defects in the double mutant are due to loss of the *ROXY1* and *ROXY2* functions.

Table 1 Frequency of aborted ovules in progeny of various crosses

Male parent	Female parent	Percentage of aborted ovules[a]	No. of counted ovules[a]
Wild-type	*roxy1-5 roxy2-2*	21.7	735
Wild-type	*roxy2-2*	2.4	642
Wild-type	Wild-type	2.4	707

[a]Ten siliques were analyzed.

Comparison of ROXY1 *and* ROXY2 *expression patterns*

In situ hybridization experiments were performed to compare *ROXY1* and *ROXY2* expression patterns in floral tissues. *ROXY1* is expressed in distinctive areas of the inflorescence apical meristem where new floral buds will be initiated. Later, strong expression is detectable in young floral organ primordia, and expression levels decrease when floral organs start to differentiate (Figure 3a; Xing *et al.*, 2005). In contrast, *ROXY2* RNA is weakly expressed throughout the whole inflorescence apical meristem and in young buds (Figure 3e). After the onset of floral organ differentiation, when archesporial cell divisions give rise to the sporogenous cells at anther stage 3 (Sanders *et al.*, 1999), overlapping expression of *ROXY1* and *ROXY2* is detectable in the four corners of young anthers (Figure 3b,f). During further differentiation, at anther stages 4 and 5, *ROXY1* and *ROXY2* are mainly expressed in PMCs formed in the center of each anther lobe and in the somatic cell layers embracing the sporogenous cells. No signals are detectable in the anther epidermis (Figure 3c,g). At stage 6, shortly before meiosis, *ROXY1* and *ROXY2* are both expressed in PMCs and in the tapetum (Figure 3d,h). After completion of meiosis, signals become restricted to the tapetum and are absent from maturing microspores (data not shown). The observation that *ROXY1* and *ROXY2* expression patterns

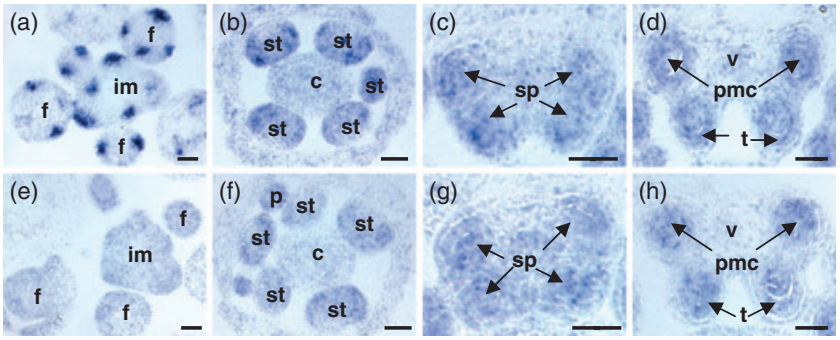

Figure 3. *In situ* hybridization analysis of *ROXY1* and *ROXY2* expression in wild-type plants.
Cross-sections through wild-type inflorescences and flowers at various stages were analyzed for *ROXY1* (a–d) and *ROXY2* (e–h) expression.
(a, e) Cross-sections through inflorescence apices, showing that *ROXY1* is strongly expressed in sepal primordia, whereas *ROXY2* is weakly expressed throughout the floral meristem.
(b, f) *ROXY1* and *ROXY2* expression overlap in young anthers at anther stage 3 in the four sectors where sporogenous and somatic cells are formed by division of archesporial cells. *ROXY2* is also weakly detectable in petal primordia.
(c, g) At anther stage 4, *ROXY1* and *ROXY2* are expressed in all four lobes of anthers, in both sporogenous cells and somatic cell layers (with the exception of the epidermis).
(d, h) Before meiosis, at anther stage 6, expression of both genes is mainly confined to PMCs and tapetum.
c, carpel; f, floral bud; im, inflorescence meristem; p, petal; pmc, pollen mother cell; sp, sporogenous cells; st, stamen; t, tapetum; v, vascular bundle. Bars = 25 μm.

coincide during early premeiotic to meiotic anther stages in sporogenous and parietal cells is in accordance with their redundant function during anther development as revealed by genetic studies.

Histological analysis of roxy1 roxy2 *anthers*

Wild-type and *roxy1-5 roxy2-2* anther development was compared by analyzing semi-thin cross-sections. Morphological differences between the double mutant and wild-type become discernable from anther stage 3 onwards, at which time primary parietal cells and primary sporogenous cells are formed in all four lobes in the wild-type. However, sporogenous cell formation fails to occur on the adaxial side of *roxy1 roxy2* anthers (Figure 4a,f). Further divisions of the primary parietal and sporogenous cells occur only in the abaxial portions of double mutant anthers at stage 5, and give rise to the three cell layers of the anther wall and the PMCs, respectively (Figure 4b,g). In the adaxial lobes, no further divisions occur, and thus no differentiation into PMCs and somatic cell layers is observed (Figure 4g). From stage 6 onwards, PMCs in the abaxial lobes adopt an aberrant shape (Figure 4c,h). Loss of *ROXY1* and *ROXY2* functions leads to a reduction in PMC callose formation, such that PMCs stick together and degenerate (Figure 4k,l). The tapetum then grows hypertrophically (Figure 4d,i) and finally degrades, leading to the formation of small, empty anther locules (Figure 4j,e).

The differential effects of *ROXY1* and *ROXY2* on abaxial and adaxial anther lobe development were further investigated by *in situ* hybridization experiments using a *SPL/NZZ* probe. *SPL/NZZ* is one of the earliest-acting anther genes and is expressed in archesporial and sporogenous cells as well as later in PMCs and tapetum (Schiefthaler *et al.*, 1999; Yang *et al.*, 1999). *SPL/NZZ* expression is detectable at anther stage 2, when archesporial cells are formed in the four corners of early wild-type and double mutant anthers (Figure 5a,e). When sporogenous cells are initiated at stage 3, expression persists in the four wild-type anther lobes (Figure 5b–d). However, in *roxy1 roxy2* double mutants, after formation of sporogenous cells in abaxial lobes at stage 3, adaxial mutant lobes are largely devoid of *SPL/NZZ* expression (Figure 5f–h). When tetrads are formed after stage 7, less *SPL/NZZ* expression is detectable in the hypertrophically growing tapetum, which is in accordance with the abnormal tapetum phenotype (Figure 5d,h). These data show that the earliest defect detectable in the double mutant specifically disrupts archesporial cell differentiation in the adaxial lobes of anthers. Later defects in the abaxial lobes are due to failure of further PMC differentiation, and could therefore also perturb meiosis.

The conserved glycine in the putative GSH binding site is crucial for ROXY1 function

Various GRXs from prokaryotes to humans are known to utilize the tripeptide glutathione (GSH) to catalyze redox-dependent functions. In the GRX catalytic cycle, GSH binds to oxidized glutaredoxin and reduces it, making the enzyme available for further reduction reactions (Fernandes and Holmgren, 2004). In addition to a conserved active site motif, a GSH binding site sequence with one conserved glycine and a few less well conserved amino acids has been described for GRXs (Fladvad *et al.*, 2005; Lundberg *et al.*, 2001; Sun *et al.*, 1998). Amino acid alignment of GRXs from *Escherichia coli* and various plant and mammalian species

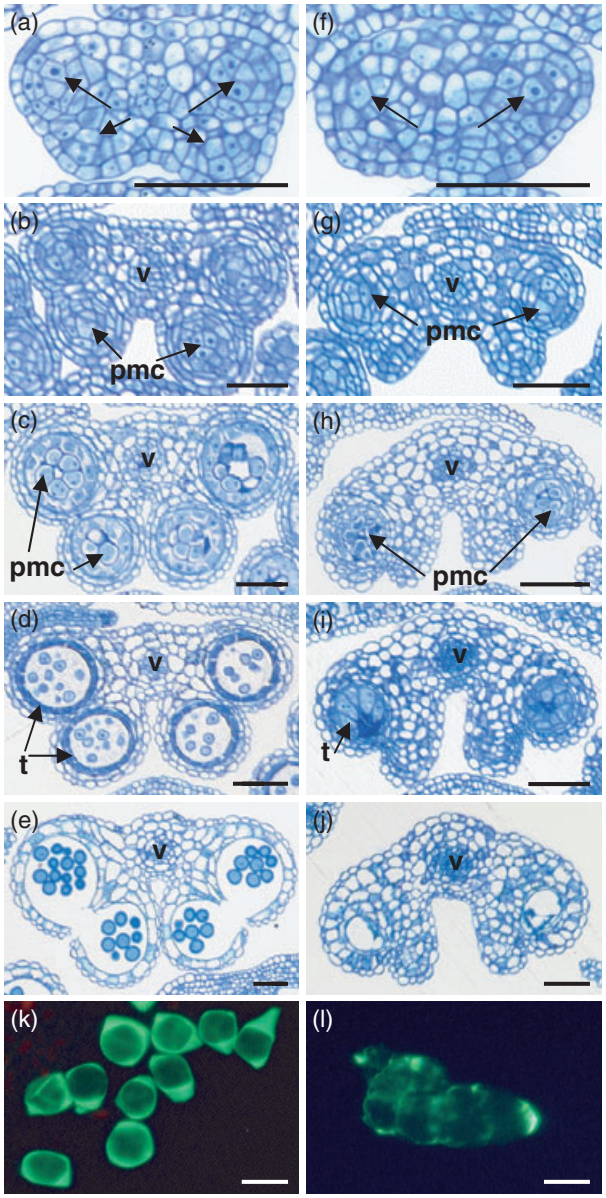

Figure 4. Comparison of wild-type and *roxy1 roxy2* anther development.
Semi-thin cross-sections through wild-type (a–e) and *roxy1 roxy2* (f–j) anthers were stained with toluidine blue.
(a) Anther stage 3. Anthers have four lobes containing sporogenous cells (arrows).
(b) Anther stage 5. The typical four-lobed anther morphology is established, and PMCs have formed in the center of each lobe.
(c) Anther stage 6. PMCs have separated and are ready to undergo meiosis.
(d) Anther stage 8. Microspores are released from the tetrads. Strong staining of the tapetum indicates its degeneration.
(e) Anther stage 13. Anthers are dehisced. Pollen sacs contain mature pollen grains, while the tapetum and middle layer have disappeared completely.
(f) Anther stage 3. Sporogenous cells have formed in abaxial anther lobes (arrows), but not in adaxial ones.
(g) Anther stage 5. Anther size is slightly reduced compared to wild-type. Two abaxial lobes are formed by somatic cells surrounding PMCs. However, no sporogenous cells are generated in the adaxial lobes.
(h) Anther stage 6. Abaxial PMCs are irregularly shaped and start to degenerate. The typical pollen sac wall is not formed in the adaxial lobes.
(i) Anther stage 8. PMCs have degenerated. The expanded tapetum occupies the anther lobe space.
(j) Anther stage 13. The tapetum is degraded and no pollen grains are detectable in the locules. A residual middle layer still exists.
(k) Wild-type PMCs separate at anther stages 6–7, and thick callose walls form (visualized by aniline blue staining).
(l) A group of PMCs from a *roxy1-5 roxy2-2* anther at stage 6. These PMCs have less callose in their walls, and therefore, unlike wild-type PMCs, remain clumped together. Bars = 50 μm in a–j; 20 μm in k,l.

revealed that this conserved glycine also exists in ROXY1 (G110) and ROXY2 (Figure 6a). To test its functional significance for a plant GRX, G110 in ROXY1 was mutated into an alanine (G110A). In addition, a conserved proline (P100) located in a conserved GRX hydrophobic surface area (Lundberg *et al.*, 2001) ten amino acids upstream of G110 was mutated (P100A, Figure 6a). The two mutated versions of *ROXY1* were expressed under the control of a 3.6 kb *ROXY1* promoter fragment that has been shown to confer endogenous *ROXY1* expression (Xing *et al.*, 2005) in *roxy1-5* plants. A wild-type version of *ROXY1* served as a control. The petal phenotype of *roxy1-5* mutants was rescued in all 40 *pROXY1::ROXY1* T_1 plants (Figure 6b,c and Figure S2). In contrast, none of the 52 *pROXY1::ROXY1m(G110A)* plants produced any wild-type flowers (Figure 6d and Figure S2). The single conserved glycine is thus crucial for rescue of the *roxy1* petal phenotype, and ROXY1 and ROXY2 probably bind GSH and use it to regenerate their reductive capacity during flower development. Mutagenesis of the conserved proline (P100A) did not prevent full complementation of 36 investigated transgenic *roxy1-5* mutants (Figure 6e and Figure S2), indicating that the hydrophobic proline is dispensable for ROXY1 function.

Structural characterization of the first plant glutaredoxin protein from poplar, the reduced Grx-C1 containing a CGYC active site (Feng *et al.*, 2006), enabled us to conduct homology modeling using Grx-C1 as a template (Figure 6f). ROXY1 and Grx-C1 share 43% sequence identity. Modeling predicts that the ROXY1 core structure is highly similar to that of Grx-C1, and shows a typical thioredoxin-fold composed of five α-helices and four β-strands (Figure 6g). This overall structure may be shared between various plant GRXs (Feng *et al.*, 2006). The conserved G110 and the CCMC active site of ROXY1 are localized on the β4-sheet and α2-helix, respectively, and both regions are localized on the protein surface, as are the corresponding amino acids in the poplar Grx-C1. Homology modeling is thus consistent with the results of mutagenesis, and suggests that ROXY1 could bind to GSH.

Expression of a large number of genes is deregulated in roxy1 roxy2 double mutants

To explore the pathways that are affected by loss of *ROXY1* and *ROXY2* activity during anther development, microarray experiments were conducted. Affymetrix 24K GeneChips were used to compare the transcriptomes of young *roxy1-5*

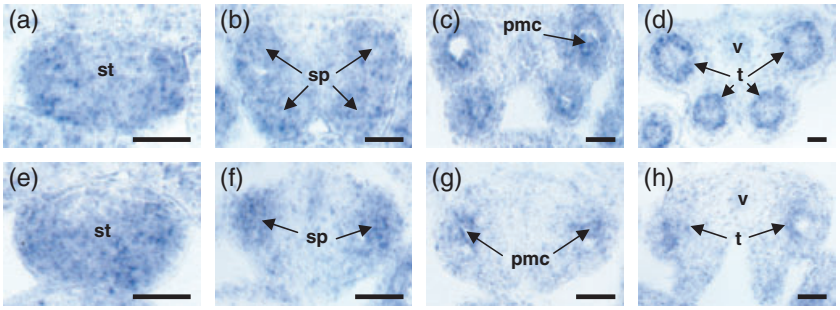

Figure 5. *In situ* hybridization analysis of *SPL/NZZ* expression in wild-type and *roxy1-5 roxy2-2* anthers.
Cross-sections through early anther stages were prepared from wild-type (a–d) and *roxy1-5 roxy2-2* (e–h) flowers.
(a, e) Anther stage 2. *SPL/NZZ* expression is detectable in the four corners of anthers, including archesporial cells, but absent from the epidermis.
(b, f) Anther stage 4. *SPL/NZZ* RNA is localized in sporogenous cells. In wild-type, the sporogenous cells in all four corners of the anther show strong expression of *SPL/NZZ* (b), whereas, in *roxy1 roxy2*, strong *SPL/NZZ* expression is restricted to the two abaxial lobes (f).
(c, g) Anther stage 6. *SPL/NZZ* is expressed within the tapetum and PMCs of all four wild-type lobes (c). In contrast, strong *SPL/NZZ* signal is only detectable in the two abaxial locules of *roxy1 roxy2* anthers (g).
(d, h) Anther stage 7. *SPL/NZZ* expression is mainly confined to the tapetum in wild-type anthers (d). A weak signal is detectable in the two abaxial locules of *roxy1-5 roxy2-2* anthers (h).
pmc, pollen mother cell; sp, sporogenous cell; st, stamen; t, tapetum; v, vascular bundle. Bars = 20 μm.

roxy2-2 and wild-type inflorescences from anther stages 1–7. The expression level of 386 genes is downregulated in the double mutant, and upregulation was observed for only 64 genes (Figure 7a and Tables S3 and S4). The largest affected group of genes belongs to the category 'other and unknown functions' (186 genes downregulated and 22 genes upregulated). Loss of *ROXY1/2* activity severely disturbs transcription of genes in the category 'metabolic function', with 60 genes downregulated and 22 genes upregulated. Further large groups of downregulated genes belong to the categories 'transcription regulation' (39 genes) and 'signal transduction' (21 genes), for which five genes and one gene, respectively, were upregulated. Loss of *ROXY1/2* activity caused downregulation of 23 redox-related genes and did not increase the transcript level of any member of this category.

RT-PCR analysis of selected genes from the array experiments confirmed differential expression in young inflorescences from wild-type and *roxy1-5 roxy2-2* plants, as well as *roxy1-4 roxy2-2* double mutants. Furthermore, it allowed us to determine effects on known anther genes such as *DYT1* (Zhang *et al.*, 2006) and *SPL8* (Unte *et al.*, 2003) that are not represented on the 24K chip. Genes identified as being downregulated in *roxy1-4 roxy2-2* were also downregulated in *roxy1-5 roxy2-2* double mutants. This downregulation was at least partially reversed in complemented *roxy1-5 roxy2-2* mutants harboring the *pROXY2::ROXY2* construct (Figure 7b). Of 33 analyzed genes, including 13 known anther genes, the expression levels of 29 were changed by factors ranging from >2 to >100 (Table 2). A correlation between the degree of expression change and the timing of gene activity during anther development was observed. The most strongly affected genes are *MS2* and *MS1*, which encode two male-sterile proteins (Aarts *et al.*, 1997; Ito and Shinozaki, 2002), for which expression was 164- and 71-fold downregulated, respectively, in the double mutant. Together with *AMS*, which was 42-fold downregulated, these anther genes act downstream of the tapetum gene *DYT1* (Ito and Shinozaki, 2002; Sorensen *et al.*, 2003; Wilson *et al.*, 2001; Zhang *et al.*, 2006). Expression of *DYT1* itself, similar to that of the transcription factor *MYB35*, was reduced over 20-fold. Expression of *A9* and *A6*, which are also known to be required for tapetum differentiation (Hird *et al.*, 1993; Paul *et al.*, 1992), were reduced to a similar extent (29- and 39-fold, respectively). Genes acting during pre-meiotic stages, such as *SPL/NZZ* and *TPD1* (Schiefthaler *et al.*, 1999; Yang *et al.*, 1999, 2003), were only slightly downregulated, about twofold. Similarly, expression of two other early-acting anther genes, *MYB33* and *MYB65*, double mutants of which fail to produce microspores and form a hypertrophic tapetum, is also slightly affected (Millar and Gubler, 2005). The callose synthase gene *CalS5* (*At2g13680*) was downregulated about fourfold, and is known to be expressed in PMCs and mature pollen (Nishikawa *et al.*, 2005), which is compatible with the observed histological defect of reduced callose formation in *roxy1-5 roxy2-2* PMCs (Figure 4l). Loss of *ROXY1/2* activity does not affect transcription of *SPL8*, which is known to control early archesporial cell formation (Unte *et al.*, 2003).

Other genes that are downregulated include genes with an unknown function, such as *At1g61070* and *At4g29980*, and also a β-1,3-glucanase, a cytochrome P450, a lipid transfer protein, an ABC transporter, a chalcone synthase, a peroxidase, an elicitor response protein and a receptor-like protein kinase (Table 2 and Figure 7b). The large variety of genes that are affected at the expression level reveals the highly complex nature of the changes caused by the simultaneous absence of *ROXY1* and *ROXY2*, supporting an important function for *ROXY1/2* in anther gene transcription.

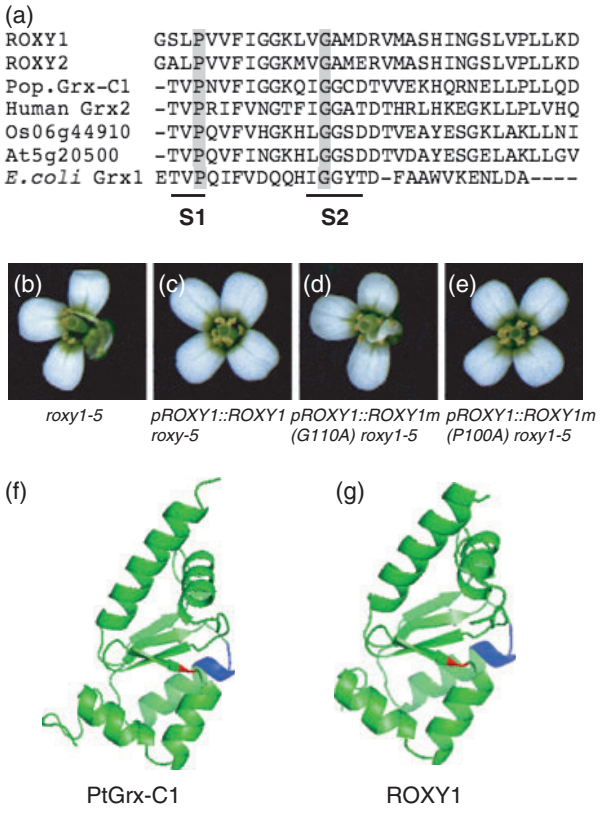

Figure 6. G110 in the putative GSH binding site is crucial for ROXY1 function.
(a) Alignment of C-terminal regions of ROXY1, ROXY2, poplar PtGrx-C1 (AAV73806), the human Grx2 (AAK72499), a rice GRX (Os06g44910), a CPYC GRX from Arabidopsis (At5g20500) and Grx1 from *E. coli* (P68688). S1 and S2 indicate a hydrophobic surface area and the GSH binding site, respectively. The positions of conserved proline and glycine residues are indicated by gray boxes; in ROXY1, these amino acids are P100 and G110, respectively.
(b) A typical *roxy1-5* flower.
(c) Flower from a T_1 *roxy1-5* plant expressing the *pROXY1::ROXY1* transgene, showing a wild-type petal phenotype.
(d) Flower from a T_1 *roxy1-5* plant expressing the *pROXY1::ROXY1m(G110A)* transgene. Replacement of the conserved Gly110 by Ala prevents rescue of the mutant petal phenotype.
(e) Flower from a *roxy1-5* T_1 plant harboring the *pROXY1::ROXY1m(P100A)* transgene. Substitution of the conserved Pro100 by Ala has no effect on the ability of ROXY1 to rescue the petal phenotype.
(f) Ribbon representation of poplar Grx-C1. Four central β-sheets are surrounded by five α-helices. The position of the conserved glycine in the GSH binding site is indicated in red, the CGYC active site is blue.
(g) Ribbon representation of ROXY1 obtained by homologous modeling using poplar Grx-C1 as a template (PDB entry 1Z7R). The conserved glycine (G110, red) and the CCMC active site (blue) are located on the same β-sheet and α-helix, respectively, as in poplar Grx-C1.
PyMOL (DeLano Scientific, Palo Alto, CA, USA; http://www.pymol.org) was used to generate Figure 6(f, g).

Discussion

Within the plant-specific Arabidopsis CC-type GRX subgroup, *ROXY1* and *ROXY2* show the highest degree of similarity to each other. Single *roxy1* mutants display a petal phenotype, whereas single *roxy2* mutants do not show any floral phenotype. However, *roxy1 roxy2* mutants are sterile and do not produce pollen. In agreement with the observed double mutant phenotypes, *ROXY1* and *ROXY2* expression domains overlap in anther primordia, PMCs and tapetum. Furthermore, expression of *ROXY2* under the control of a *ROXY1* promoter fragment can fully rescue the *roxy1* mutant phenotype (unpublished data), demonstrating that *ROXY2* can substitute for *ROXY1* in petal development. These findings show an important redundant function for *ROXY1* and *ROXY2* in anther development.

ROXY1 *and* ROXY2 *affect abaxial and adaxial anther lobe development differentially*

Loss of the *ROXY1/2* functions impairs sporogenous cell formation in adaxial lobes, indicating an indispensable early adaxial anther function for *ROXY1* and *ROXY2*. However, in abaxial anther lobes, sporogenous and somatic cell formation proceeds further without requiring *ROXY1/2* activity. Therefore, the *roxy1 roxy2* double mutant produces only two visible abaxial pollen sacs. Some 3500 Arabidopsis genes may be specifically expressed in the anther and contribute to anther cell differentiation and cell fate (Scott *et al.*, 2004). Several anther mutants have been isolated from Arabidopsis and maize, most of which affect later stages of anther cell differentiation. In the *spl/nzz* mutant, the four anther lobes are simultaneously affected (Schiefthaler *et al.*, 1999; Yang *et al.*, 1999). In contrast, in *spl8* mutants, microsporogenesis does occur occasionally, but with equal probability in all locules within the anther (Unte *et al.*, 2003). Similarly, the maize *msca1* mutant also shows defects in archesporial cell division (Chaubal *et al.*, 2003). The differential *roxy1 roxy2* anther phenotype could be due to early *ROXY1/2* targets being unequally expressed or functioning in anther lobes. Alternatively, other redundantly acting GRXs or redox modulators might exist that function differentially during early anther development.

ROXY1 *and* ROXY2 *contribute to tapetum development*

In the abaxial sectors of double mutant anthers, degeneration of PMCs is accompanied by hypertrophic growth of the tapetum, and tapetal cells eventually occupy most of the locule space. A functional tapetum is crucial for pollen development as it provides nutrients and enzymes for the developing PMCs (Scott *et al.*, 2004). Although entry into meiosis can occur in the absence of a normal tapetal cell layer, as observed in *gne2* mutants (Sorensen *et al.*, 2002), several tapetum-defective mutants show a male-sterile phenotype. In *myb33 myb65* double mutants, PMCs degenerate due to tapetum hypertrophy, which begins early, at the pre-meiotic stage (Millar and Gubler, 2005). The *myb33 myb65* phenotype seems to be conditional, as high

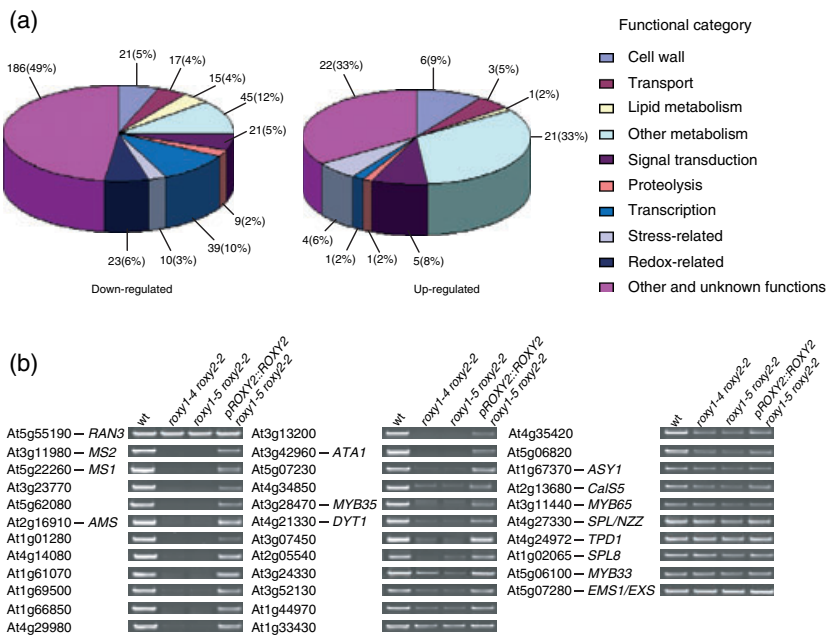

Figure 7. Expression analysis of deregulated genes in *roxy1 roxy2* double mutant.
(a) Functional classification of the deregulated genes identified by comparing wild-type and *roxy1-5 roxy2-2* double mutant young inflorescences using the Affymetrix 24K GeneChip. Lists of downregulated and upregulated genes are provided in Tables S3 and S4, respectively.
(b) Representative RT-PCR data for selected genes from the microarray experiment and selected known anther genes that are not present on the Affymetrix 24K GeneChip. RT-PCR was performed for wild-type, *roxy1-4 roxy2-2* and *roxy1-5 roxy2* mutants, and transgenic plants harboring the *pROXY2::ROXY2* transgene in a *roxy1-5 roxy2-2* background. Primers used for the PCR are listed in Table S2.

light intensities and low temperature can restore male fertility (Millar and Gubler, 2005); no such environmental effect was observed in *roxy1 roxy2* mutants (data not shown). Other mutants, such as *fat tapetum* and *gne1*, also exhibit a hypertrophic tapetum, but, unlike *roxy1 roxy2* and *myb33 myb65,* these mutants also display excessive growth of the middle layer (Sanders *et al.*, 1999; Sorensen *et al.*, 2002). Tapetal hypertrophy in *roxy1 roxy2* mutants is probably a direct consequence of the absence of *ROXY1* and *ROXY2*, as both genes are normally expressed in this cell layer. The tapetal effect is accompanied by delayed degeneration of the tapetal cell, a process that is considered to be a programmed cell death event (Papini *et al.*, 1999). These data imply that plant GRXs participate in the modulation of signaling pathways leading to tapetal cell death, which might contribute to the defects observed during further abaxial PMC differentiation.

ROXY1 *and* ROXY2 *probably require interaction with GSH for their function*

The mechanistic basis of GRX activity has been intensively studied in *E. coli*, yeast and mammals, and binding of GSH is known to be required for the action of these enzymes. A GSH binding site has been identified in GRXs, and comprises a conserved glycine, flanked by less well-conserved amino acids (Fladvad *et al.*, 2005; Sun *et al.*, 1998). Substitution of Ala for the conserved G110 in ROXY1 destroys its ability to complement the *roxy1* phenotype (Figure 6d), proving that the conserved glycine is also essential for the function of this plant CC-type GRX. Given the sequence similarity between ROXY1 and ROXY2 and their functional redundancy, it seems likely that both proteins act as oxidoreductases and regenerate their reductive capacities via interaction with GSH, mediated by the conserved glycine.

Homologous protein modeling, using the NMR solution structure of Grx-C1 from poplar as a template (Feng *et al.*, 2006), shows that ROXY1 and also ROXY2 (data not shown) most probably form a typical thioredoxin-fold structure, composed of central β-sheets surrounded by α-helices. The conserved glycine and the crucial N-terminal cysteine of the active site motif are both located on the surface of the predicted protein structure, and are thus available for interaction with other molecules. Reduced levels of GSH are known to affect flowering time and root development in Arabidopsis (Cobbett *et al.*, 1998; Ogawa *et al.*, 2004), and this key component of plant antioxidant defenses seems to also have a function in various developmental processes, probably in conjunction with GRXs.

A model for ROXY1/2 *function in anther development*

Based on our genetic and expression data, we provide a model for *ROXY1/2* function during anther development (Figure 8e). The putative transcription factor *SPL/NZZ* is required for sporogenous anther cell formation. *spl/nzz* mutant anthers lack endothecium, middle layer, tapetum and meiocytes in all four lobes (Schiefthaler *et al.*, 1999; Yang *et al.*, 1999). As the anther phenotype of the *spl-1 roxy1 roxy2* triple mutant resembles that of the *spl-1* single mutant (Figure 8a,b), and no strong *SPL-1* expression changes were determined in the double mutant, the two GRXs probably act downstream of *SPL/NZZ*. The tapetum

Table 2 Quantification of effects on expression for selected downregulated genes in *roxy1 roxy2* inflorescences

AGI accession	Gene symbol	Fold change	Gene annotation
At3g11980	*MS2*	164.6 ± 2.7	Male-sterile protein 2
At5g22260	*MS1*	71.4 ± 0.8	Male-sterile protein 1
At3g23770		49.3 ± 0.2	β-1,3-glucanase
At5g62080		48.8 ± 0.3	A9 protein precursor-like protein
At2g16910	*AMS*	42.6 ± 0.4	bHLH transcription factor
At1g01280		42.0 ± 1.8	Cytochrome P450
At4g14080		39.3 ± 0.4	A6 anther-specific protein
At1g61070		38.6 ± 0.5	Unknown protein
At1g69500		37.9 ± 0.3	Cytochrome P450
At1g66850		37.6 ± 0.6	Lipid transfer protein
At4g29980		37.5 ± 0.1	Hypothetical protein
At3g13200		35.7 ± 0.3	ABC transporter
At3g42960	*ATA1*	31.6 ± 0.5	Alcohol dehydrogenase
At5g07230		29.7 ± 0.2	A9 protein
At4g34850		29.1 ± 0.4	Chalcone synthase-like protein
At3g28470	*MYB35*	27.2 ± 0.7	MYB transcription factor
At4g21330	*DYT1*	22.3 ± 0.2	bHLH transcription factor
At3g07450		20.8 ± 0.6	Putative 5B anther-specific protein
At2g05540		11.7 ± 0.2	Putative glycine protein
At3g24330		11.2 ± 0.3	β-1,3-glucanase
At3g52130		9.6 ± 0.4	5B-like protein, cysteine-rich protein
At1g44970		9.0 ± 0.1	Peroxidase
At1g33430		8.3 ± 0.2	Elicitor response protein
At4g35420		7.6 ± 0.2	Putative dihydroflavonol-4-reductase
At5g06820		7.3 ± 0.2	Receptor-like protein kinase
At1g67370	*ASY1*	5.2 ± 0.2	Meiotic asynaptic mutant 1
At2g13680	*CalS5*	4.2 ± 0.2	Callose synthase
At3g11440	*MYB65*	2.1 ± 0.1	MYB transcription factor
At4g27330	*SPL/NZZ*	2.0 ± 0.1	*SPOROCYTELESS/NOZZLE*
At4g24972	*TPD1*	1.9 ± 0.1	*TAPETUM DETERMINANT 1*
At5g06100	*MYB33*	1.4 ± 0.1	MYB transcription factor
At1g02065	*SPL8*	1.1 ± 0.1	*SPL8* transcription factor
At5g07280	*EMS1/EXS*	1.1 ± 0.1	*EXCESS MICROSPOROCYTES1/EXTRA SPOROGENOUS CELLS*

Total RNA for semi-quantitative RT-PCR was isolated from inflorescences harvested from wild-type (Nössen) and *roxy1-5 roxy2-2* double mutants. Mean fold changes are indicated, ±standard deviation.

regulator *DYT1* was suggested to function downstream of *SPL/NZZ* (Zhang *et al.*, 2006). Our expression analysis shows that *DYT1*, as well as its targets *MS1*, *AMS* and *MYB35*, are strongly downregulated in *roxy1 roxy2* double mutants. Furthermore, the *dyt1 roxy1 roxy2* triple mutant phenotypically resembles the *roxy1 roxy2* double mutant (Figures 4j and 8c,d). Together, these data imply that *ROXY1/2* acts upstream of *DYT1*, regulating tapetum differentiation and thereby probably affecting PMC meiosis and further microspore development. However, we cannot exclude the possibility that *ROXY1/2* exert a direct function in PMC differentiation, which is supported by the fact that both genes are expressed in PMCs. Expression profiling studies revealed that a large variety of genes are affected at the transcriptional level in the double mutant. The observed correlation between the onset of anther gene expression and the strength of their downregulation in the double mutant may serve as a starting point to predict the position of more genes in the early anther regulatory pathway and to investigate their functions.

To conclude, the plant-specific glutaredoxins *ROXY1* and *ROXY2* require a conserved glycine interacting with GSH for modification of target proteins. Environmental stress is known to decrease plant fertility, and gametophyte development is highly sensitive to stress and reactive oxygen species (Ambrus *et al.*, 2006; Sun *et al.*, 2004). Mutagenesis studies have suggested that conserved cysteines in MYB R2R3 proteins mediate their redox-dependent ability to bind to promoter sequences (Heine *et al.*, 2004), and thus these proteins might represent targets for post-translational modification by ROXY1 and ROXY2. Further analysis of these plant glutaredoxins should shed light on the importance of redox control in normal anther development and plant fertility.

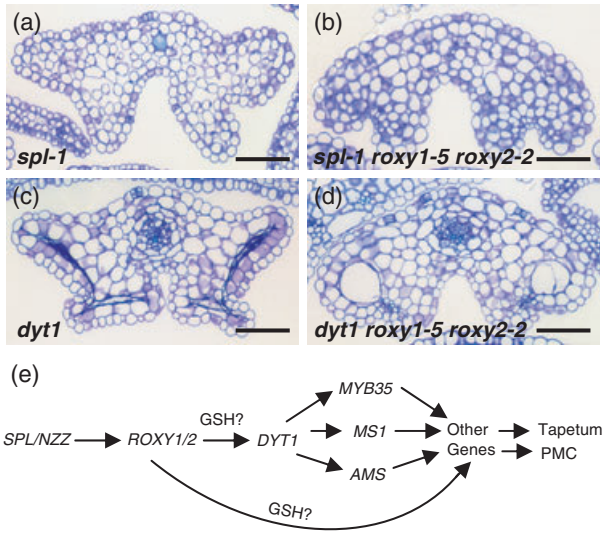

Figure 8. Mutant anther morphology and model for *ROXY1/2* function in anther development.
(a–d) Cross-sections of mutant anthers at stage 12. (a) *spl-1*. (b) *spl-1 roxy1-5 roxy2-2*. (c) *dyt1*. (d) *dyt1 roxy1-5 roxy2-2*. (e) Arrows indicate positive genetic regulation between the genes. GSH, glutathione. Bars = 50 μm.

Experimental procedures

Growth of plants and isolation of mutants

Plants were grown in the greenhouse at 21–23°C under long-day conditions (16 h light). *roxy2-1* and *roxy2-2* mutants were isolated from the SIGnAL T-DNA collection (line SALK_057273, Col-0) and from the RIKEN Ds insertions collection (line 13-1723-1, Nössen; Ito *et al.*, 2002; Kuromori *et al.*, 2004), respectively. Homozygous mutants were identified by PCR genotyping. For *roxy2-1*, gene-specific primers 5′-AGCCGACAAGAAGGATAGATATATCC-3′and 5′-ACGCATCACTCTTCTCTCTCACTGTC-3′ were used. The T-DNA insertion was detected using the left border primer 5′-GCGT GGACCGCTTGCTGCAACT-3′ and the gene-specific reverse primer. Gene-specific primers for *roxy2-2* were 5′-AAAGCTAGCAACCAT-GATGGTCC-3′and 5′-GTTAACATTTATATATTAGTGTG-3′. The *Ds* primer 5′-TCCGTTCCGTTTTCGTTTTTTAC-3′ was used in combination with the reverse gene-specific primer to detect the insertion. Two new *ROXY1* alleles in the Nössen background, *roxy1-4* and *roxy1-5*, were obtained from the RIKEN Ds collection (lines 11-2698-1 and 13-1220-1). The homozygocity of mutants displaying petal abnormalities was confirmed using the *ROXY1* primers 5′-CAGAGTTAGACTCAGAGGTGTAGTAGG-3′ and 5′-GAATAG ATACGGCGTCAGTTAATACCG-3′. For *roxy1-4*, the reverse *ROXY1* primer was combined with the Ds primer 5′-CCGGATCG-TATCGGTTTTCG-3′, and, for *roxy1-5*, the reverse *ROXY1* primer was used together with the Ds primer 5′-TCCGTTCCGTTTTCG TTTTTTAC-3′.

spl-1 (N6586, The European Arabidopsis Stock Centre) and *dyt1* (line 15-3398-1, RIKEN) mutants were identified by phenotype screening and genotyping. The gene-specific primer (5′-TGTT-CTTCATCAATCTCAGGAGGAGCTTC-3′) and Ds primer (5′-CCGGAT-CGTATCGGTTTTCG-3′) were used for detecting the Ds insertion in *dyt1*, while the gene-specific primer pair 5′-TCGAAATGTTACCATTC-CTTTGTCTG-3′ and 5′-ATCGAGATTTGGGACTTACGTTGGTG-3′ was used to confirm *dyt1* homozygocity.

Crosses and mutant phenotype analysis

Various *roxy1* alleles were crossed to *roxy2-2*. Sterile double mutant phenotypes in a F_2 population were confirmed by genotyping. Reciprocal crosses were performed to test for effects on male and/or female fertility. Siliques from crosses were harvested and dissected 8 days after pollination to determine the number of aborted ovules under a binocular microscope (Leica MZ-FLIII; http://www.leica-microsystems.com). To generate *spl-1 roxy1-5 roxy2-2* and *dyt1 roxy1-5 roxy2-2* triple mutants, *spl-1* (+/–) and *dyt1* (+/–) hemizygotes, respectively, were crossed with *roxy1-5 roxy2-2* double mutants, and F_2 plants were phenotypically screened and genotyped. For microscopic examination, young floral buds from anther stages 2–13 were processed as described by Sorensen *et al.* (2002). For analysis of the callose wall, PMCs were stained with 0.1% aniline blue at anther stage 6. Samples were photographed under a Zeiss Axiophot microscope (http://www.zeiss.com/) using a digital camera (JVC KY-F75U; http://www.jvc-victor.co.jp).

Transgenic plant construction

To test whether *ROXY2* can complement the *roxy1-5 roxy2-2* phenotype, a 4440 bp genomic fragment was amplified by PCR using the primers 5′-GCGGATCCTTTCAGGTAAACATCTCATTGATAGTG-3′ and 5′-ACGGATCCACCTGTTGGCGTCTTTCTGTTCATCATC-3′, and cloned into the binary vector pGSA1252. After sequence verification, the binary vector was transformed into *Agrobacterium* strain GV3101. Transgenic plants were generated by transformation of *roxy2-2* –/– *roxy1-5* –/+ plants.

To generate the *ROXY1* promoter construct, a 3.6 kb region located immediately upstream of the *ROXY1* start codon was amplified from Col-0 genomic DNA (adding appropriate restriction sites to facilitate cloning), using the primer pair 5′-GCGTAGATCT-CAATAGTCGAGGATCATTCGGAGTGC-3′ and 5′-ATGCCCATGGTC-TAGATTTGATATCTCTTCTCTTTCTCTTGTTAC-3′. The resulting product was cloned into the binary vector pGSA1252. Point mutations at specific positions in the *ROXY1* coding sequence were created using a PCR-based technique as described by Xing *et al.* (2005). To introduce the P100A and G110A mutations, pairs of mutagenic oligomers were used (5′-AGGGTCTCTCgCGGTCGTCTT-CATC-3′ and 5′-ATGAAGACGACCGcGAGAGACCCTG-3′ for P100A, 5′-ACTGGTTGcAGCTATGGACAGAGTCATGG-3′ and 5′-AGCCAT GACTCTGTCCATAGCTgCAACCAG-3′ for G110A; mutated bases are indicated in lower case). After sequencing, the wild-type version or the two mutated *ROXY1* genes were fused to the 3.6 kb *ROXY1* promoter and the constructs were transformed into *roxy1-5* mutants. Transgenic T_1 plants were tested for complementation of the *roxy1* phenotype.

In situ *RNA hybridization*

In situ hybridization was performed as previously described, using PCR templates containing binding sites for the T3 or T7 RNA polymerase (Zachgo, 2002). The *ROXY1* antisense probe was prepared according to the method described by Xing *et al.* (2005). To avoid cross-hybridization with *ROXY1*, the *ROXY2* antisense probe was prepared using a unique 160 bp fragment from the 5′ end of *ROXY2* (5′-CAACCAACTCTCACACAAATTCTC-3′ and 5′-CGGCAATTAAC-CCTCACTAAAGGGCACCTTACTGTTGTTG-3′) and a unique 220 bp fragment from the 3′ end of *ROXY2* (5′-ATCAATGG-CTCACTCGTCCC-3′ and 5′-CGGCAATTAACCCTCACTAAAGGGGA-CAAAGAGCTAAGC-3′) as templates. For *SPL/NZZ* antisense probe production, a template was used that comprised the whole

coding region sequence, and was amplified using the primers 5′- GCGGAATTAACCCTCACTAAAGGGATCAATGGCGACTTCTCTC TTCTTC-3′ and 5′-GCTCGTAATACGACTCACTATAGGGCTTAAA GCTTCAAGGACAAATCAATGG-3′.

Homology modeling

Comparative modeling was performed using the automated Swiss-MODEL server (accessible via the ExPASy web server at http://swissmodel.expasy.org//SWISS-MODEL.html), which uses ProMod for three-dimensional protein modeling. Grx-C1 from poplar (1Z7RA) was used as the model as it shows the highest homology to ROXY1 (43%) among available templates. This allowed modeling of ROXY1 amino acids 21-136.

Isolation of total RNA and semi-quantitative RT-PCR

Total RNA was isolated from young inflorescences comprising apical meristems and young flower buds up to flower stage 10 (as defined by Smyth *et al.*, 1990) obtained from wild-type (Nössen), *roxy1-5 roxy2-2* and *roxy1-4 roxy2-2* double mutants and T_1 plants harboring the *pROXY2::ROXY2* transgene in a *roxy1-5 roxy2-2* background, using the RNeasy Plant Mini Kit (Qiagen, http://www.qiagen.com/). For semi-quantitative RT-PCR, 4 μg aliquots of total RNA were treated with RNase-free DNase I (Roche; http://www.roche-applied-science.com), and SuperScript™ II reverse transcriptase (Invitrogen, http://www.invitrogen.com/) was used to produce first-strand cDNA according to the manufacturer's instructions. Aliquots of 5 μl from 25 μl reactions were loaded on an ethidium bromide-stained 1.0% w/v agarose gel. Bands were quantified by scanning gels using the phosphor imager Typhoon 8600 (Amersham Biosciences, http://www5.amershambiosciences.com/), using Image Quant version 5.2 software (Amersham Biosciences). *Ran3* (*At5g55190*) was used for normalization of signal strength and as a reference for expression levels. Three RT-PCR repetitions were conducted for each gene, and primer pairs are listed in Table S2.

Microarray analysis

Three biological samples for total RNA were prepared from wild-type (Nössen) and the *roxy1-5 roxy2-2* double mutant, respectively, as described for semi-quantitative RT-PCR. Probe preparation, hybridization to ATH1 Arabidopsis Genome Arrays (Affymetrix, Santa Clara, California; http://www.affymetrix.com) and statistical data analysis were carried out at the Integrated Functional Genomic service unit (University of Münster, Germany; http://ifg-izkf.uni-muenster.de). Data processing was performed using Affymetrix microarray suite 5.0. Only genes with an expression ratio (fold change, down or up) ≥2.0 and *P*-values <0.01 were considered. Functional classification of deregulated genes was performed manually, based on established and putative functions (TAIR, http://www.arabidopsis.org).

Acknowledgements

We thank Anja Hörold for excellent assistance and Dr Maren Heese for support with homology modeling. We also thank Dr Peter Huijser and Dr Andrea Busch for commenting on the manuscript. S.Z. is grateful to Professor Heinz Saedler for ongoing support and stimulating discussions. This work was supported by a grant from the Deutsche Forschungsgemeinschaft to S.Z. (ZA 259/4-1).

Supplementary Material

The following supplementary material is available for this article online:

Figure S1. A 4440 bp *ROXY2* genomic fragment complements the sterility phenotype of the *roxy1-5 roxy2-2* double mutant.

Figure S2. RT-PCR analysis of mutagenized *ROXY1* expression levels in transgenic plants.

Table S1. Type and number of reproductive organs in second and third whorls of *roxy1* and *roxy2* flowers.

Table S2. Primer pairs used for semi-quantitative RT-PCR.

Table S3. List of 386 downregulated genes in the *roxy1-5 roxy2-2* double mutant.

Table S4. List of 64 upregulated genes in the *roxy1-5 roxy2-2* double mutant.

This material is available as part of the online article from http://www.blackwell-synergy.com

Please note: Blackwell Publishing are not responsible for the content or functionality of any supplementary materials supplied by the authors. Any queries (other than missing material) should be directed to the corresponding author for the article.

References

Aarts, M.G., Hodge, R., Kalantidis, K., Florack, D., Wilson, Z.A., Mulligan, B.J., Stiekema, W.J., Scott, R. and Pereira, A. (1997) The Arabidopsis MALE STERILITY 2 protein shares similarity with reductases in elongation/condensation complexes. *Plant J.* **12**, 615–623.

Albrecht, C., Russinova, E., Hecht, V., Baaijens, E. and de Vries, S. (2005) The *Arabidopsis thaliana SOMATIC EMBRYOGENESIS RECEPTOR-LIKE KINASES1* and *2* control male sporogenesis. *Plant Cell*, **17**, 3337–3349.

Ambrus, H., Darko, E., Szabo, L., Bakos, F., Kiraly, Z. and Barnabas, B. (2006) In vitro microspore selection in maize anther culture with oxidative-stress stimulators. *Protoplasma*, **228**, 87–94.

Buchanan, B.B. and Balmer, Y. (2005) Redox regulation: a broadening horizon. *Annu. Rev. Plant Biol.* **56**, 187–220.

Canales, C., Bhatt, A.M., Scott, R. and Dickinson, H. (2002) *EXS*, a putative LRR receptor kinase, regulates male germline cell number and tapetal identity and promotes seed development in Arabidopsis. *Curr. Biol.* **12**, 1718–1727.

Chaubal, R., Anderson, J.R., Trimnell, M.R., Fox, T.W., Albertsen, M.C. and Bedinger, P. (2003) The transformation of anthers in the msca1 mutant of maize. *Planta*, **216**, 778–788.

Cobbett, C.S., May, M.J., Howden, R. and Rolls, B. (1998) The glutathione-deficient, cadmium-sensitive mutant, *cad2-1*, of *Arabidopsis thaliana* is deficient in gamma-glutamylcysteine synthetase. *Plant J.* **16**, 73–78.

Colcombet, J., Boisson-Dernier, A., Ros-Palau, R., Vera, C.E. and Schroeder, J.I. (2005) Arabidopsis *SOMATIC EMBRYOGENESIS RECEPTOR KINASES1* and *2* are essential for tapetum development and microspore maturation. *Plant Cell*, **17**, 3350–3361.

Feng, Y., Zhong, N., Rouhier, N., Hase, T., Kusunoki, M., Jacquot, J.P., Jin, C. and Xia, B. (2006) Structural insight into poplar glutaredoxin C1 with a bridging iron-sulfur cluster at the active site. *Biochemistry*, **45**, 7998–8008.

Fernandes, A.P. and Holmgren, A. (2004) Glutaredoxins: glutathione-dependent redox enzymes with functions far beyond a simple thioredoxin backup system. *Antioxid. Redox Signal.* **6**, 63–74.

Fladvad, M., Bellanda, M., Fernandes, A.P., Mammi, S., Vlamis-Gardikas, A., Holmgren, A. and Sunnerhagen, M. (2005) Molec-

ular mapping of functionalities in the solution structure of reduced Grx4, a monothiol glutaredoxin from *Escherichia coli*. *J. Biol. Chem.* **280**, 24553–24561.

Heine, G.F., Hernandez, J.M. and Grotewold, E. (2004) Two cysteines in plant R2R3 MYB domains participate in redox-dependent DNA binding. *J. Biol. Chem.* **279**, 37878–37885.

Hird, D.L., Worrall, D., Hodge, R., Smartt, S., Paul, W. and Scott, R. (1993) The anther-specific protein encoded by the *Brassica napus* and *Arabidopsis thaliana A6* gene displays similarity to β-1,3-glucanases. *Plant J.* **4**, 1023–1033.

Hord, C.L.H., Chen, C., DeYoung, B.J., Clark, S.E. and Ma, H. (2006) The *BAM1/BAM2* receptor-like kinases are important regulators of Arabidopsis early anther development. *Plant Cell*, **18**, 1667–1680.

Ito, T. and Shinozaki, K. (2002) The *MALE STERILITY1* gene of Arabidopsis, encoding a nuclear protein with a PHD-finger motif, is expressed in tapetal cells and is required for pollen maturation. *Plant Cell Physiol.* **43**, 1285–1292.

Ito, T., Motohashi, R., Kuromori, T., Mizukado, S., Sakurai, T., Kanahara, H., Seki, M. and Shinozaki, K. (2002) A new resource of locally transposed dissociation elements for screening gene-knockout lines in silico on the Arabidopsis genome. *Plant Physiol.* **129**, 1695–1699.

Kuromori, T., Hirayama, T., Kiyosue, Y., Takabe, H., Mizukado, S., Sakurai, T., Akiyama, K., Kamiya, A., Ito, T. and Shinozaki, K. (2004) A collection of 11800 single-copy Ds transposon insertion lines in Arabidopsis. *Plant J.* **37**, 897–905.

Lemaire, S.D. (2004) The glutaredoxin family in oxygenic photosynthetic organisms. *Photosynth. Res.* **79**, 305–318.

Lundberg, M., Johansson, C., Chandra, J., Enoksson, M., Jacobsson, G., Ljung, J., Johansson, M. and Holmgren, A. (2001) Cloning and expression of a novel human glutaredoxin (Grx2) with mitochondrial and nuclear isoforms. *J. Biol. Chem.* **276**, 26269–26275.

Ma, H. (2005) Molecular genetic analyses of microsporogenesis and microgametogenesis in flowering plants. *Annu. Rev. Plant Biol.* **56**, 393–434.

Millar, A.A. and Gubler, F. (2005) The Arabidopsis *GAMYB*-like genes, *MYB33* and *MYB65*, are microRNA-regulated genes that redundantly facilitate anther development. *Plant Cell*, **17**, 705–721.

Nishikawa, S., Zinkl, G.M., Swanson, R.J., Maruyama, D. and Preuss, D. (2005) Callose (beta-1,3 glucan) is essential for Arabidopsis pollen wall patterning, but not tube growth. *BMC Plant Biol.* **7**, 5–22.

Ogawa, K., Hatano-Iwasaki, A., Yanagida, M. and Iwabuchi., M. (2004) Level of glutathione is regulated by ATP-dependent ligation of glutamate and cysteine through photosynthesis in *Arabidopsis thaliana*: mechanism of strong interaction of light intensity with flowering. *Plant Cell Physiol.* **45**, 1–8.

Papini, A., Mosti, S. and Brighigna, L. (1999) Programmed-cell-death events during tapetum development of angiosperms. *Protoplasma*, **207**, 213–221.

Paul, W., Hodge, R., Smartt, S., Draper, J. and Scott, R. (1992) The isolation and characterisation of the tapetum-specific *Arabidopsis thaliana A9* gene. *Plant Mol. Biol.* **19**, 611–622.

Rouhier, N., Couturier, J. and Jacquot, J.P. (2006) Genome-wide analysis of plant glutaredoxin systems. *J. Exp. Bot.* **57**, 1685–1696.

Sanders, P.M., Bui, A.Q., Weterings, K., McIntire, K.N., Hsu, Y.C., Lee, P.Y., Truong, M.T., Beals, T.P. and Goldberg, R.B. (1999) Anther developmental defects in *Arabidopsis thaliana* male-sterile mutants. *Sex. Plant Reprod.* **11**, 297–322.

Schiefthaler, U., Balasubramanian, S., Sieber, P., Chevalier, D., Wisman, E. and Schneitz, K. (1999) Molecular analysis of *NOZZLE*, a gene involved in pattern formation and early sporogenesis during sex organ development in *Arabidopsis thaliana*. *Proc. Natl Acad. Sci. USA*, **96**, 11664–11669.

Scott, R.J., Spielman, M. and Dickinson, H.G. (2004) Stamen structure and function. *Plant Cell*, **16**, S46–S60.

Smyth, D.R., Bowman, J.L. and Meyerowitz, E.M. (1990) Early flower development in Arabidopsis. *Plant Cell*, **2**, 755–767.

Sorensen, A., Guerineau, F., Canales-Holzeis, C., Dickinson, H.G. and Scott, R.J. (2002) A novel extinction screen in *Arabidopsis thaliana* identifies mutant plants defective in early microsporangial development. *Plant J.* **29**, 581–594.

Sorensen, A.M., Kröber, S., Unte, U.S., Huijser, P., Dekker, K. and Saedler, H. (2003) The Arabidopsis *ABORTED MICROSPORES* (*AMS*) gene encodes a MYC class transcription factor. *Plant J.* **33**, 413–423.

Sun, C., Berardi, M.J. and Bushweller, J.H. (1998) The NMR solution structure of human glutaredoxin in the fully reduced form. *J. Mol. Biol.* **280**, 687–701.

Sun, K., Hunt, K. and Hauser, B.A. (2004) Ovule abortion in Arabidopsis triggered by stress. *Plant Physiol.* **135**, 2358–2367.

Unte, U.S., Sorensen, A., Pesaresi, P., Gandikota, M., Leister, D., Saedler, H. and Huijser, P. (2003) *SPL8*, an SBP-box gene that affects pollen sac development in Arabidopsis. *Plant Cell*, **15**, 1009–1019.

Wilson, Z.A., Morroll, S.M., Dawson, J., Swarup, R. and Tighe, P.J. (2001) The Arabidopsis *MALE STERILITY1* (*MS1*) gene is a transcriptional regulator of male gametogenesis, with homology to the PHD-finger family of transcription factors. *Plant J.* **28**, 27–39.

Xing, S., Rosso, M.G. and Zachgo, S. (2005) *ROXY1*, a member of the plant glutaredoxin family, is required for petal development in *Arabidopsis thaliana*. *Development*, **132**, 1555–1565.

Xing, S., Lauri, A. and Zachgo, S. (2006) Redox regulation and flower development: a novel function for glutaredoxins. *Plant Biol.* **8**, 547–555.

Yang, W.C., Ye, D., Xu, J. and Sundaresan, V. (1999) The *SPOROCYTELESS* gene of Arabidopsis is required for initiation of sporogenesis and encodes a novel nuclear protein. *Genes Dev.* **13**, 2108–2117.

Yang, S., Xie, L., Mao, H., Puah, C.S., Yang, W., Jiang, L., Sundaresan, V. and Ye, D. (2003) *TAPETUM DETERMINANT1* is required for cell specialization in the Arabidopsis anther. *Plant Cell*, **15**, 2792–2804.

Zachgo, S. (2002) *In situ* hybridization. In *Molecular Plant Biology* (Gilmartin, P.M. and Blower, C., eds). Oxford, UK: Oxford University Press, pp. 41–63.

Zhang, W., Sun, Y., Timofejeva, L., Chen, C., Grossniklaus, U. and Ma, H. (2006) Regulation of Arabidopsis tapetum development and function by *DYSFUNCTIONAL TAPETUM1 (DYT1)* encoding a putative bHLH transcription factor. *Development*, **133**, 3085–3095.

Zhao, D., Wang, G., Speal, B. and Ma, H. (2002) The *EXCESS MICROSPOROCYTES1* gene encodes a putative leucine-rich repeat receptor protein kinase that controls somatic and reproductive cell fates in the Arabidopsis anther. *Genes Dev.* **16**, 2021–2031.

